









RESEARCH ARTICLE

Identification of novel modulators of a schistosome transient receptor potential channel targeted by praziquantel

Evgeny G. Chulkov¹ , Emery Smith² , Claudia M. Rohr¹ , Nawal A. Yahya^{1,3} , Sang-Kyu Park¹ , Louis Scampavia² , Timothy P. Spicer² , Jonathan S. Marchant^{1*} 

1 Department of Cell Biology, Neurobiology and Anatomy, Medical College of Wisconsin, Milwaukee, Wisconsin, United States of America, **2** Department of Molecular Medicine, Scripps Research, Jupiter, Florida, United States of America, **3** Department of Pharmacology, University of Minnesota Medical School, Minneapolis, Minnesota, United States of America

 These authors contributed equally to this work.

* JMMarchant@mcw.edu



OPEN ACCESS

Citation: Chulkov EG, Smith E, Rohr CM, Yahya NA, Park S-K, Scampavia L, et al. (2021) Identification of novel modulators of a schistosome transient receptor potential channel targeted by praziquantel. *PLoS Negl Trop Dis* 15(11): e0009898. <https://doi.org/10.1371/journal.pntd.0009898>

Editor: Robert M. Greenberg, University of Pennsylvania, UNITED STATES

Received: June 17, 2021

Accepted: October 11, 2021

Published: November 3, 2021

Copyright: © 2021 Chulkov et al. This is an open access article distributed under the terms of the [Creative Commons Attribution License](https://creativecommons.org/licenses/by/4.0/), which permits unrestricted use, distribution, and reproduction in any medium, provided the original author and source are credited.

Data Availability Statement: All data are in the manuscript and its [supporting information](#) files.

Funding: This work was supported by NIH R01-AI145871 and R01-AI155405 (to JSM), NIH F31-AI145091 (to NAY) and the Marcus Family (to JSM). This work was also supported in part by a NIH S10 instrument award (1S100D025282-01) that provided Scripps Research with the FLIPR Tetra system integrated into HTS operations (to TPS,LS). The funders had no role in study design,

Abstract

Given the worldwide burden of neglected tropical diseases, there is ongoing need to develop novel anthelmintic agents to strengthen the pipeline of drugs to combat these burdensome infections. Many diseases caused by parasitic flatworms are treated using the anthelmintic drug praziquantel (PZQ), employed for decades as the key clinical agent to treat schistosomiasis. PZQ activates a flatworm transient receptor potential (TRP) channel within the melastatin family (TRPM_{PZQ}) to mediate sustained Ca²⁺ influx and worm paralysis. As a druggable target present in many parasitic flatworms, TRPM_{PZQ} is a promising target for a target-based screening campaign with the goal of discovering novel regulators of this channel complex. Here, we have optimized methods to miniaturize a Ca²⁺-based reporter assay for *Schistosoma mansoni* TRPM_{PZQ} (*Sm*.TRPM_{PZQ}) activity enabling a high throughput screening (HTS) approach. This methodology will enable further HTS efforts against *Sm*.TRPM_{PZQ} as well as other flatworm ion channels. A pilot screen of ~16,000 compounds yielded a novel activator of *Sm*.TRPM_{PZQ}, and numerous potential blockers. The new activator of *Sm*.TRPM_{PZQ} represented a distinct chemotype to PZQ, but is a known chemical entity previously identified by phenotypic screening. The fact that a compound prioritized from a phenotypic screening campaign is revealed to act, like PZQ, as an *Sm*.TRPM_{PZQ} agonist underscores the validity of TRPM_{PZQ} as a druggable target for antischistosomal ligands.

Author summary

The drug praziquantel is used to treat diseases caused by parasitic flatworms. Praziquantel is an old drug, and there is a need to identify novel treatments that retain desirable features and improve weaknesses in the mode of PZQ action. One way to do this is to identify new drugs that exploit vulnerabilities in the same drug target but work in slightly

data collection and analysis, decision to publish, or preparation of the manuscript.

Competing interests: The authors have declared that no competing interests exist.

differently ways. Here, we have optimized high throughput screening methods to pharmacologically profile a parasitic flatworm ion channel targeted by PZQ. We have identified several new chemical structures that interact with this channel complex. These ligands provide new opportunity for developing tools to manipulate flatworm biology and potentially new trajectories for anthelmintic drug development.

Introduction

Over a billion people worldwide require chemotherapy for neglected tropical diseases (NTDs, [1]). Schistosomiasis, a disease caused by infection by parasitic flatworms known as schistosomes, is one of several NTDs targeted for elimination as a public health problem in the World Health Organization 2021–2030 NTD road map [1]. Schistosomiasis, as well as several other parasitic flatworm infections [2], are treated using the anthelmintic drug praziquantel (PZQ). PZQ has remained an effective treatment for schistosomiasis over four decades of clinical use [3], underpinning recent mass drug administration (MDA) campaigns aimed at decreasing infections and morbidity in vulnerable populations. Alternatives to PZQ are however needed. PZQ has several features that could be improved and the threat of drug resistance, potentially accelerated by the rollout of MDA initiatives, persists [4–6].

We recently discovered that PZQ activates a Ca^{2+} -permeable ion channel in *Schistosoma mansoni* that belongs to the melastatin family of transient receptor potential (TRP) channels (christened *Sm*.TRPM_{PZQ} [7,8]). PZQ also acts a potent activator of TRPM_{PZQ} in other PZQ-sensitive parasites [9]. TRP channels, which act as non-selective cation channels, are appealing targets for anthelmintic drug discovery owing both to their important physiological roles in sensory physiology as well as their druggability [10–15]. However, little is currently known about the pharmacology of flatworm TRP channels. Efforts to profile these channels will be important for validating tools to selectively manipulate worm physiology, as well as for anthelmintic development [13–15]. Insight to date suggests schistosome TRP channels, like other flatworm targets [16], exhibit a different pharmacological profile compared with their closest mammalian counterparts. For example, *Schistosoma mansoni* TRPA1 responds to capsaicin, a human TRPV ligand [17]. *Sm*.TRPM_{PZQ}, which harbors a TRPM8-like binding pocket in the voltage-sensor like domain (transmembrane helices S1-S4, [9]), is not activated by the human TRPM8 agonists menthol and icilin [7]. Customization of these TRP channels to parasite-specific functions may underpin this divergence and specialization.

To characterize flatworm TRP channel pharmacology, it would be helpful to establish methods for screening individual channels against diverse drug libraries. *Sm*.TRPM_{PZQ} is a good candidate for optimizing such an approach given it is targeted by PZQ, and mediates a large, sustained Ca^{2+} signal in heterologously expressing cells. In collaboration with the Molecular Screening Center at Scripps Research in Florida, we optimized target-based screening approaches for *Sm*.TRPM_{PZQ} with the goal of discovering other ligands that engage this ion channel complex [18]. The hope is that by optimizing high-throughput screening (HTS) methods for TRPM_{PZQ}, new chemotypes distinct from PZQ can be identified including ligands that act at different sites on the channel relative to the transmembrane PZQ-binding pocket [9]. These could include allosteric modulators, or ligands that interact with the pore-forming domain (S5-S6). Such ‘hits’ could then be further iterated and evaluated as leads for anthelmintic development.

Here, we executed a pilot screen of ~16,000 compounds against *Sm*.TRPM_{PZQ} which identified numerous antagonists as well as a single novel activator of *Sm*.TRPM_{PZQ}. Interestingly

this *Sm*.TRPM_{PZQ} activator is a known chemical entity previously prioritized from a phenotypic screen of schistosome worms. These data underscore first, the feasibility of a high throughput screening (HTS) approach for flatworm TRP channels, and second convergence of target- and phenotype-based screening approaches on the same ligand here revealed to act as a *Sm*.TRPM_{PZQ} agonist.

Results

Activation of *Sm*.TRPM_{PZQ} heterologously expressed in HEK293 cells was resolved by following changes in fluorescence emission of a synthetic Ca²⁺ indicator over time [7]. In cells, transiently expressing *Sm*.TRPM_{PZQ} and seeded into a 96-well plate, addition of \pm PZQ (3 μ M) caused a rapid, dose-dependent increase in fluorescence (Fig 1A, [7]). Addition of higher concentrations of PZQ (\leq 30 μ M) to untransfected HEK293 cells failed to elicit any change in basal fluorescence (Fig 1A, [7]).

In order to support a large scale HTS, we trialed various conditions to support miniaturization of this basic reporter assay into smaller volumes necessary for screening in 1536-well format. Miniaturization of the screening assay was aided by the large amplitude of the *Sm*.TRPM_{PZQ}-dependent Ca²⁺ transient (change of fluorescence/basal fluorescence, $\Delta F/F = 12.3 \pm 2.1$ for PZQ signals at *Sm*.TRPM_{PZQ} versus $\Delta F/F = 4.5 \pm 1.5$ for ATP signals through endogenous receptors as measured by confocal Ca²⁺ imaging [7]) and the non-desensitizing nature of the PZQ-evoked Ca²⁺ signal, which was sustained over several minutes (Fig 1A). Experimental performance was compared (i) using various densities of *Sm*.TRPM_{PZQ}-transfected cells assayed in suspension, (ii) at different temperatures (room temperature (RT) versus 37°C), and (iii) using either freshly transfected cells, or thawed stocks of previously frozen transfected cells. Each condition was trialed in a 1,536 well format using the fluorescent dye calcium-5 (K_d for Ca²⁺ = 390 nM). Assay performance under these screening conditions was compared by calculating the Z' factor (Z'), a widely used indicator of HTS assay robustness [19], as well as by monitoring the dynamic range of the assay (signal[F_{max}]:basal[F_{basal}], S:B). Z' values over 0.5 are considered to be a prerequisite for an excellent HTS.

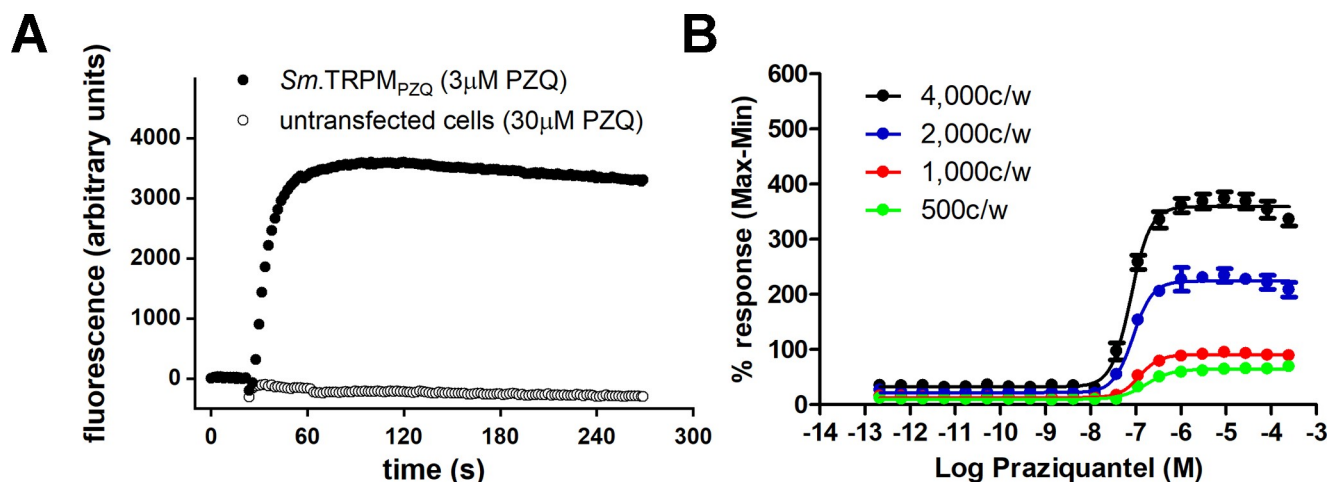


Fig 1. Optimization of assay conditions for monitoring *Sm*.TRPM_{PZQ} activity. (A) Representative fluorescence trace showing the kinetics of the Ca²⁺ signal resulting from addition of PZQ (3 μ M) to HEK293 cells transiently expressing *Sm*.TRPM_{PZQ} (closed symbols), or addition of a higher concentration of PZQ (30 μ M) to untransfected HEK293 cells (open symbols). (B) Concentration response curves of PZQ-stimulated Ca²⁺ signals in *Sm*.TRPM_{PZQ} expressing HEK293 cells resolved at various densities of cells per well (c/w) measured in suspension in 1,536 well plates at room temperature. Each point on each curve represents the average of responses from 16 replicates which were also run in 2 separate experiments to achieve average and standard deviation.

<https://doi.org/10.1371/journal.pntd.0009898.g001>

Assays in the 1536 well format demonstrated that increasing the cell count per well resulted in increased signal and dynamic range (Fig 1B), as well as a decrease in the measured EC_{50} (from 135 ± 15 nM at 1000 cells/well, to 79 ± 2 nM at 4000 cells/well, Table 1). The temperature at which responses were recorded (RT versus 37°C) did not change the sensitivity of *Sm*. $TRPM_{PZQ}$ under these assay conditions (Table 1). Optimal conditions for executing the assay were selected as 4000 cells/well in suspension at room temperature, where assay performance exceeded needed parameters (Table 1). Similar assay performance was achieved using either fresh cells ($EC_{50} = 79\pm 2$ nM, $Z' = 0.82\pm 0.03$, S:B = 10.05 ± 0.08 , Table 1) or thawed cells from previously frozen stocks ($EC_{50} = 90\pm 10$ nM, $Z' = 0.86\pm 0.02$, S:B = 10.55 ± 0.08) under the same assay conditions. Therefore, to further minimize assay variation, pilot screens were all performed using a single batch of transfected cells prepared in bulk and then frozen. This facilitated execution of screens and removed transfection efficiency as an experimental variable. Data from all of these trials are summarized in Table 1.

After optimizing conditions for miniaturization into a 1,536 well format, we proceeded to execute a screening campaign against a total of 15,984 compounds. The screened libraries comprised LOPAC₁₂₈₀ (1280 compounds), the Pathogen Box (400 compounds) and a subset of the in-house Scripps Drug Discovery Library, which included the Maybridge Hitfinder library. The screening pipeline consisted of (i) a primary, fixed concentration screen (5 μM) performed in triplicate in both ‘agonist’ and ‘antagonist’ mode, followed by (ii) titration and finally (iii) counter-screening assays of all putative ‘hits’. For the primary screen, following compound addition and completion of the ‘agonist’ (AG) mode read of 3 minutes, the ‘antagonist’ (ANT) mode commenced by PZQ addition (at an EC_{80} concentration) to wells that contain either compounds or DMSO (‘low control’). The output was compared to the response of wells with DMSO without PZQ stimulation (‘high control’). A summary of the workflow and observed compound attrition through each of these steps is shown schematically in Fig 2. Single point scatterplots from all compounds tested in the primary screen are shown in Fig 3.

Assay performance in the primary agonist screen met quality thresholds ($Z' = 0.71\pm 0.04$, S:B = 11.40 ± 0.04) and the observed sensitivity to PZQ was consistent with the prior assay optimization trials (EC_{50} for PZQ = 101 ± 3 nM). Assay performance in the primary antagonist screen also met quality thresholds ($Z' = 0.72\pm 0.04$, S:B = 9.4 ± 0.4). Hit cut-offs for both screening modes was determined using an interval-based algorithm [20,21]. The sample field in the agonist screen was taken as a percentage response (‘hit-cutoff’ >16%) which identified 181 putative ‘hits’ for further progression. The initial sample field in the antagonist screen was calculated as a ‘hit-cutoff’ >36%, which identified 188 putative ‘hits’ for further evaluation.

A total of 368 compounds were then advanced to titration screening from the primary screen ‘agonist’ and ‘antagonist’ assays (1 compound was not commercially available). Each of

Table 1. Assay metrics under specified conditions. EC_{50} , Z' and S:B were determined for *Sm*. $TRPM_{PZQ}$ activation by PZQ at indicated cell densities and temperatures. Conditions in bold text indicate the final conditions selected for the screen. For each condition, responses were found to be positively cooperative (Hill coefficients range of 1.5–2).

Cell density	Temperature	EC_{50} (nM)	Z'	S:B
500 c/w	RT	195 ± 25	0.31 ± 0.37	5.55 ± 0.73
500 c/w	37°C	202 ± 4	0.44 ± 0.14	7.28 ± 0.28
1000 c/w	RT	135 ± 15	0.48 ± 0.07	5.73 ± 0.06
1000 c/w	37°C	144 ± 2	0.53 ± 0.08	7.41 ± 0.01
2000 c/w	RT	95 ± 7	0.69 ± 0.04	8.23 ± 0.17
2000 c/w	37°C	108 ± 2	0.79 ± 0.03	8.04 ± 0.39
4000 c/w	RT	79 ± 2	0.82 ± 0.03	10.05 ± 0.08
4000 c/w	37°C	80 ± 1	0.83 ± 0.01	9.24 ± 1.23

<https://doi.org/10.1371/journal.pntd.0009898.t001>

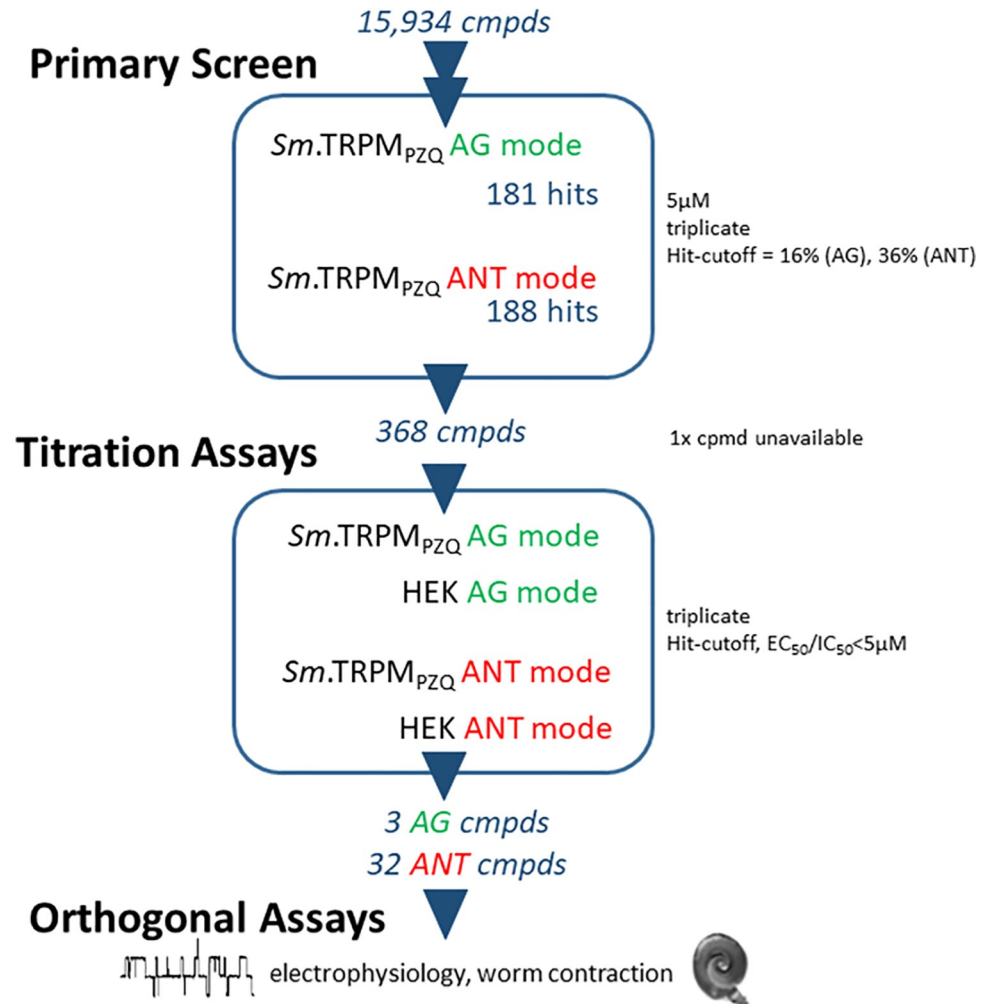


Fig 2. *Sm.TRPM_{pZQ}* screening pipeline. All HTS assays were performed in 1,536 well format. A fixed concentration (nominally 5 μM) primary screen was followed by titration assays and counter-screening in untransfected HEK cells. All assays were performed in triplicate in both agonist (AG) and antagonist (ANT) mode. From the original 15,934 compounds (*cmpds*) screened, the pipeline yielded 3 putative agonist ‘hits’ (two hits were identified as PZQ present as a ligand in the screened libraries) and 32 putative antagonist ‘hits’. Selected compounds were validated using electrophysiology and by monitoring contraction of schistosome worms *ex vivo*.

<https://doi.org/10.1371/journal.pntd.0009898.g002>

these 368 compounds was profiled as a 10-point dose-response analysis run in triplicate against untransfected HEK cells (‘counterscreen’) as well as HEK cells expressing *Sm.TRPM_{pZQ}*. Assay performance in these titration assays met required specifications (S1 Table). After curve-fitting, compounds displaying an $EC_{50} > 5 \mu M$ (agonist) or $IC_{50} > 5 \mu M$ (antagonist) were considered ‘inactive’ and not studied further. The surviving ‘hits’ that progressed through this pipeline comprised 3 potential agonists and 32 potential antagonists. Full details of these hits and associated assay data are provided in S2 and S3 Tables.

All three agonist hits were evaluated in further detail. Two of the agonist hits were identified from the Pathogen Box, and one from LOPAC1280. The primary screening data and titration analysis from the plates containing these compounds were extracted from the screening dataset. Two of these hits were identified as PZQ (red symbols, Fig 4A) as both the Pathogen Box and LOPAC1280 libraries contained PZQ as a test ligand. A third agonist ‘hit’ (christened

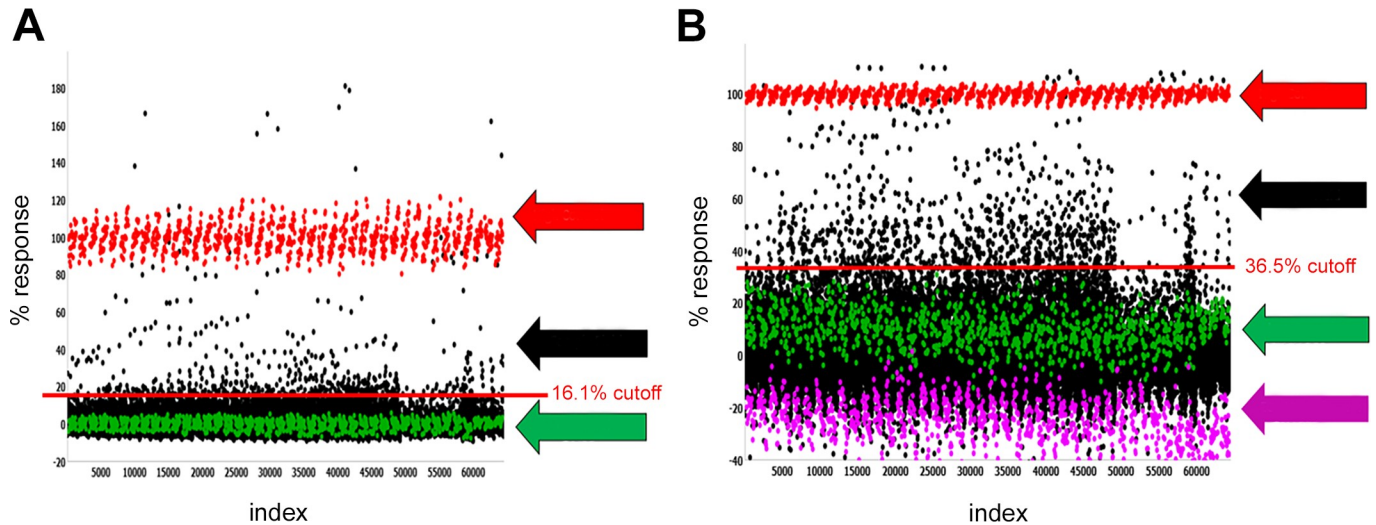


Fig 3. Primary HTS assay data. Scatterplot of all 15,934 compounds tested in (A) agonist mode and (B) antagonist mode. Each dot graphed represents the activity of a well containing test compound (black, sample field) or controls (red high control; green, low control). Arrows (right) indicated the high control (red), low control (green) and the sample field (black, datapoints between the calculated cutoffs (red lines) and high control). For the agonist screen, high control reflected responses to PZQ (10 μ M, red) and the low control represented responses to DMSO (green). For the antagonist screen, the high control reflected responses to DMSO (red) and the low control represented responses to submaximal PZQ (500 nM, green). The response to a maximal PZQ concentration (EC_{MAX} , 10 μ M) is also indicated (magenta). The EC_{80} stimulation is qualified as a percentage of the response to the high control PZQ EC_{100} (EC_{MAX}). All plates are assessed for robustness with $Z' > 0.5$ and EC_{stim} between 70–95%.

<https://doi.org/10.1371/journal.pntd.0009898.g003>

'AG1', blue circle), from the Pathogen Box, elicited strong activation of *Sm*.TRPM_{PZQ} ($B_{max} = 93.9 \pm 5.6\%$) in the primary screen (Fig 4A). AG1 is a known chemical entity (3-(3,4-dimethoxyphenyl)-6-(3-(propan-2-yl)phenyl)-[1,2,4]triazolo[4,3-a]pyridine, MMV688313; Fig 4A) and represents a chemotype distinct from PZQ. Addition of AG1 (100 μ M) resulted in a sustained cytoplasmic Ca^{2+} signal in cells expressing *Sm*.TRPM_{PZQ} resembling the action of PZQ (compare Fig 4B with Fig 1A). AG1 action was also assessed against a *Sm*.TRPM_{PZQ} channel mutant (*Sm*.TRPM_{PZQ}[R1514A]) in the fourth transmembrane spanning helix (TM4) that blocks PZQ action by ablating interactions necessary to shape the PZQ binding pocket [9]. As expected, PZQ did not elevate Ca^{2+} in cells expressing *Sm*.TRPM_{PZQ}[R1514A] (Fig 4B). However, this binding site mutant also ablated AG1 activity (Fig 4B), suggesting that AG1 also acts as an orthosteric ligand. Concentration-response curve analysis revealed AG1 acted as a full agonist of *Sm*.TRPM_{PZQ} ($EC_{50} = 1.6 \pm 0.3 \mu$ M) in Ca^{2+} flux assays, with no activity observed on counter-screening in naïve HEK cells (Fig 4C). The potency of AG1 was lower than observed with either sample of PZQ (EC_{50} s of 177 ± 21 nM, 619 ± 225 nM) present in two libraries screened under identical conditions (Fig 4C). Both ligands were then re-sourced for validation assays and activities were re-assessed from independently procured samples (PZQ, $EC_{50} = 406$ nM; AG1, $EC_{50} = 9.2 \mu$ M). Finally, the action of AG1 was studied against adult schistosome worms isolated from infected mice. Addition of AG1 to schistosome worms *ex vivo* evoked a sustained contraction (Fig 4D), although the kinetics of onset of the AG1-evoked contraction were slower than observed with PZQ. Collectively, these data identify AG1, a distinct chemical entity from PZQ, as a novel *Sm*.TRPM_{PZQ} agonist.

Screening in antagonist mode identified several 32 potential blockers of *Sm*.TRPM_{PZQ} (S2 Table). To begin analysis of this larger set of ligands, we investigated that action of one of the more potent blockers, the compound ANT1 (1-(9H-fluoren-9-yl)-4-(5-methyl-3-phenyl-1,2-oxazole-4-carbonyl)piperazine, Fig 4E). ANT1 blocked PZQ-evoked Ca^{2+} signals (IC_{50} of $1.3 \pm 0.3 \mu$ M) mediated by *Sm*.TRPM_{PZQ} (Fig 4F). When applied to intact worms ANT1 did not

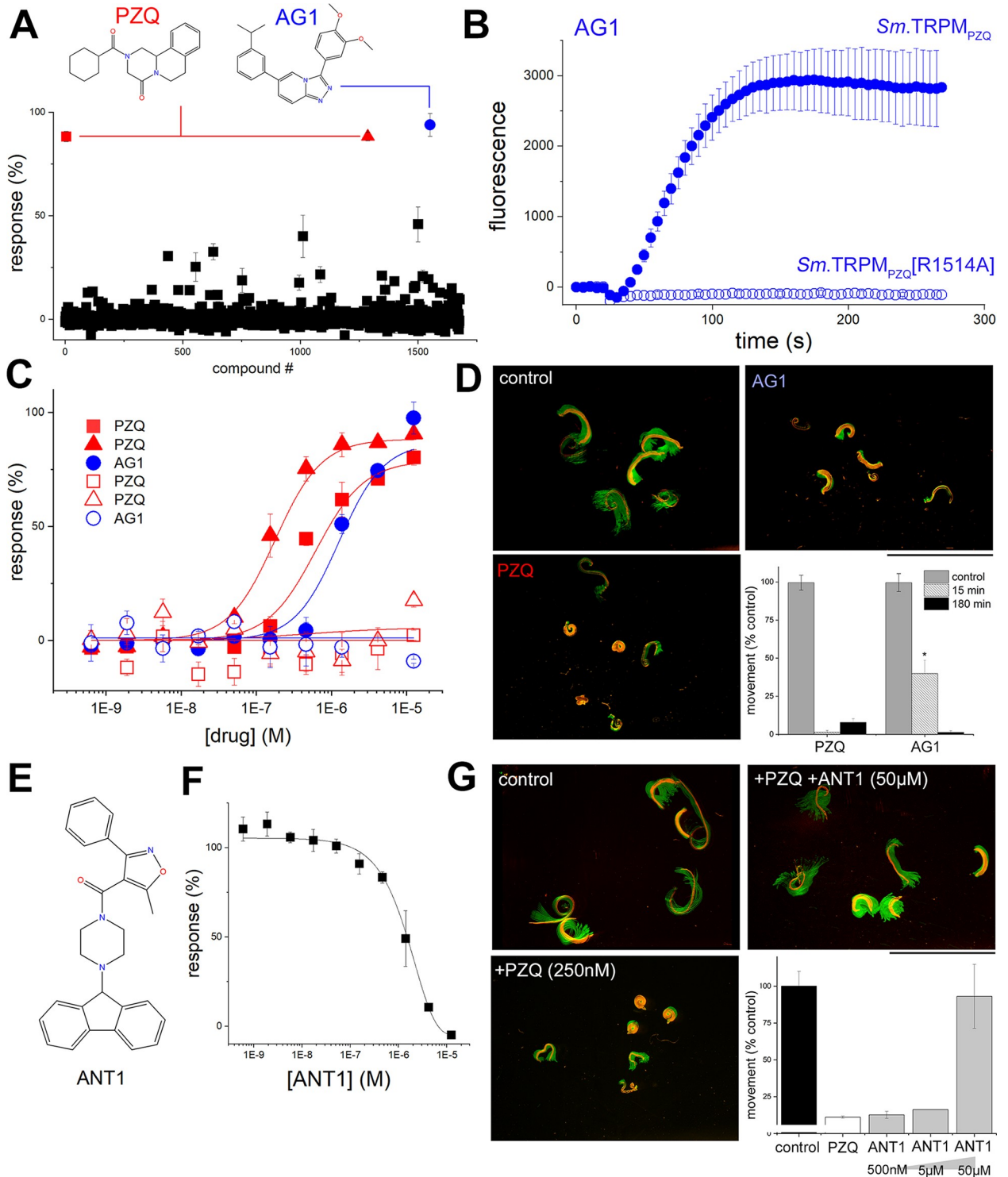


Fig 4. Identification of new chemotypes active at *Sm.TRPM_{PZQ}*. (A) Primary screen of *Sm.TRPM_{PZQ}* in agonist mode measuring peak Ca^{2+} signal amplitude in response to 1,678 compounds (LOPAC₁₂₈₀, Pathogen Box) tested at 5 μ M final concentration. Structures of 'hits' (PZQ, red; AG1, blue) are shown. (B) Kinetics of a response of wild-type *Sm.TRPM_{PZQ}* to AG1 (30 μ M, closed circles), or the binding pocket mutant *Sm.TRPM_{PZQ}[R1514A]* to AG1 (open circles). (C) Analysis of the three primary screen hits via full concentration response curves for PZQ (compounds #5, #1287) and AG1 (compound #1552) in HEK293 cells transiently transfected with *Sm.TRPM_{PZQ}* (solid symbols) or untransfected controls (open). Data represent mean \pm sd of triplicate samples. (D) Images of adult schistosome worms with single frame image (red) overlaid with maximum intensity projection (green) of a time-lapse series to illustrate worm movement and effects of PZQ (500 nM) and AG1 (1 μ M) on worm

motion 15 mins after treatment. Graph shows effects of drugs on worm motility after a 15 min and 180 min exposure (*, $p < 0.01$). Data are analyzed from $n \geq 3$ independent infections. (E) Structure of a putative *Sm*.TRPM_{PZQ} blocker (ANT1) from HTS screening activities. (F) Concentration-dependent blockade of *Sm*.TRPM_{PZQ} dependent Ca^{2+} signals (evoked by 500 nM PZQ) by increasing concentrations of ANT1. (G) Images of adult schistosome worms with single frame image (red) overlaid with maximum intensity projection of a time-lapse series to illustrate worm movement (green) and the effect of PZQ (250 nM) as well as PZQ in the presence of ANT1 (50 μ M). Data are captured after 24 hours of incubation. *Inset*, quantitative analysis of data from $n = 3$ independent infections.

<https://doi.org/10.1371/journal.pntd.0009898.g004>

change worm motility, but at high concentrations (50 μ M) enhanced recovery of schistosome worms incubated in the continued presence of PZQ compared to worms treated with PZQ alone (Fig 4G).

To validate ANT1 using an orthogonal assay, ANT1 action versus PZQ and AG1 was assessed using an electrophysiological approach. Single channel recordings of *Sm*.TRPM_{PZQ} activity were made in Ca^{2+} -free buffer following addition of either PZQ or AG1 (10 μ M) to a cell-free patch in 'inside-out' recording mode. Both PZQ and AG1 evoked step-wise openings of *Sm*.TRPM_{PZQ} (Fig 5A) with channel activation defined by linear I-V relationship in response to both agonists (Fig 5B). The mean slope single-channel conductance for PZQ- and AG1- activated *Sm*.TRPM_{PZQ} was 76 ± 8 and 61 ± 4 pS respectively (mean \pm SD). Addition of PZQ, or AG1, evoked sustained, non-desensitizing *Sm*.TRPM_{PZQ} currents, which were blocked by subsequent addition of ANT1 in a time-dependent manner (Fig 5C). Analysis of single channel open probability (P_{open}) from these records demonstrated ANT1 decreased P_{open} at *Sm*.TRPM_{PZQ} channels activated by either agonist (Fig 5D). After ANT1 application, brief channel openings persisted in the presence of PZQ or AG1 that were not seen in the presence of PZQ after addition of the pore blocker La^{3+} [7]. This observation is again suggestive of a competitive interplay between ANT1 and the channel activators, PZQ or AG1, within the orthosteric binding pocket of *Sm*.TRPM_{PZQ}.

In summary, these data reveal that AG1 behaves a novel activator of *Sm*.TRPM_{PZQ} and ANT1 as a blocker of PZQ (or AG1) action at *Sm*.TRPM_{PZQ}. Both these ligands have structures different from PZQ, evidencing the druggability of *Sm*.TRPM_{PZQ} by novel chemotypes.

Discussion

Here, we report successful miniaturization of a reporter assay (6 μ l assay volume) to monitor the activity of a parasitic flatworm ion channel, *Sm*.TRPM_{PZQ}. This approach will enable further HTS campaigns to provide insight about the properties and regulation of this recently discovered flatworm ion channel that is targeted by PZQ [8,9]. Critically, the ability to screen diverse libraries provides opportunity to discover new chemotypes active at this channel complex. This is important as the structure-activity relationship of PZQ has long been known be 'tight' with even minor modifications to the ligand causing a marked decrease in activity [9]. This has frustrated efforts to rationally engineer PZQ derivatives with enhanced properties, or improved metabolic stability. Alternative chemotypes to PZQ are required, both to mitigate some of the deficiencies of this stalwart therapeutic, as well as to bolster the global drug development pipeline [4]. Our knowledge of the properties of the PZQ binding site in TRPM_{PZQ} derive from recent mutagenesis and modeling studies guided by analyses of responses to PZQ and related derivatives [9]. However, an expansive body of work on the human TRPM8 channel evidences accommodation of various chemotypes within a malleable transmembrane binding pocket [22,23], that overlaps with the binding site for PZQ characterized in *Sm*.TRPM_{PZQ} [9]. Indeed (S)-PZQ engages this binding pocket in hTRPM8 [24,25]. Such data justify screening for new chemotypes active at flatworm TRPM_{PZQ} channels.

For these reasons, we optimized methods to allow a pilot screen of ~16,000 compounds at *Sm*.TRPM_{PZQ}. After titration and counter-screening, a single novel activator of *Sm*.

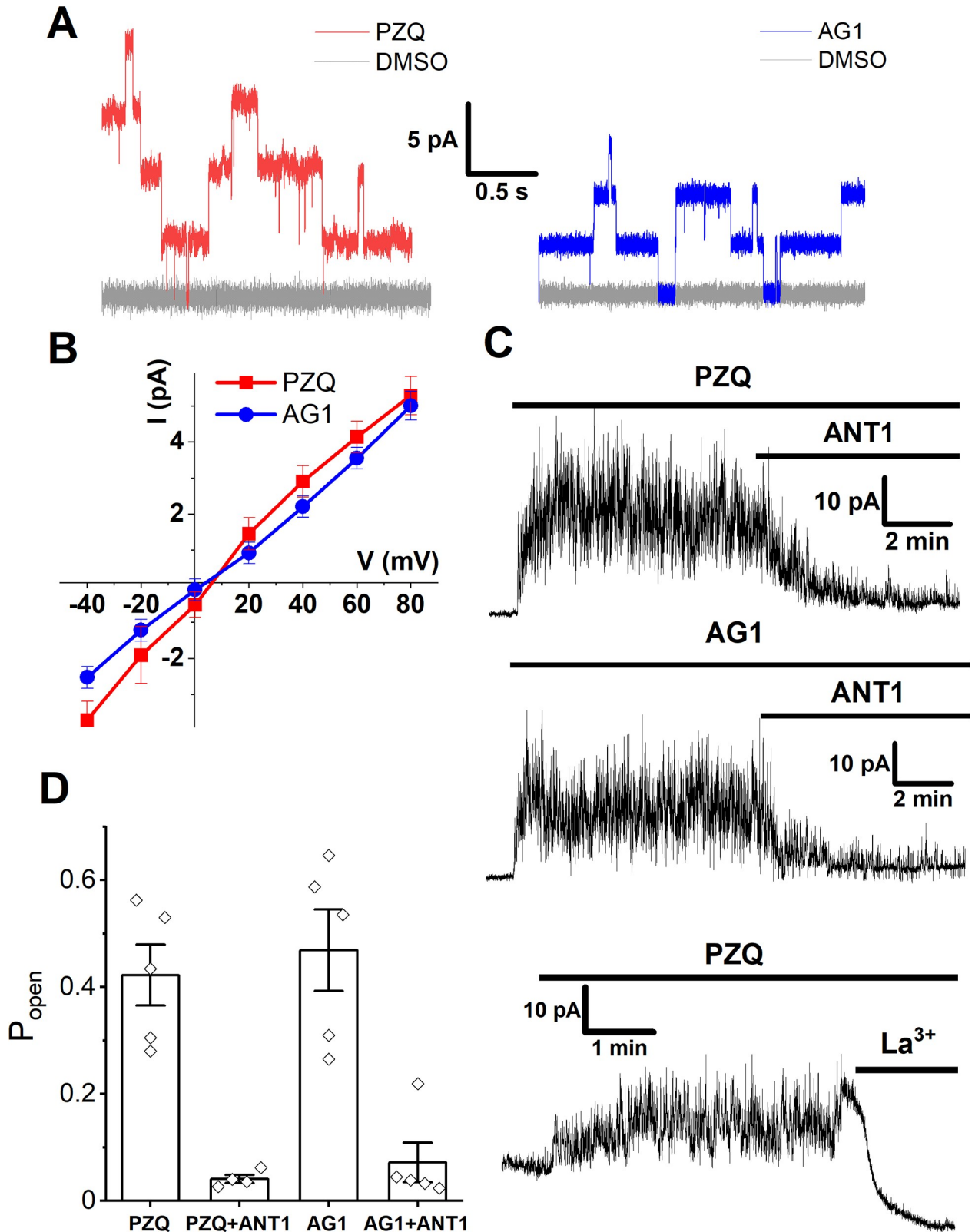


Fig 5. Electrophysiological analysis of new *Sm*.TRPM_{PZQ} chemotypes. (A) *Sm*.TRPM_{PZQ} channel fluctuations evoked by PZQ (red) or AG1 (blue) both applied at 10 μ M compared to vehicle responses (grey, 0.1% DMSO). Recordings were made in Ca²⁺-free solution at a clamping potential of +60mV in an inside-out configuration. DMSO and the test drug (PZQ or AG1) were added sequentially to the same patch. (B) Current

(I)-voltage (V) relationship of *Sm*.TRPM_{PZQ} activated with PZQ (10 μM, red) or AG1 (10 μM, blue). (C) Effect of ANT1 (top and middle, 50 μM) or La³⁺ (bottom, 10 mM) addition on *Sm*.TRPM_{PZQ} activity evoked by PZQ (10 μM) or AG1 (10 μM) measured in cell-free mode at +40mV using an inside-out configuration. (D) Measurements of single channel open probability (P_{open}) under the indicated conditions. Welch's t-test: PZQ vs 'PZQ+ANT1', $p = 0.002$; AG1 vs 'AG1+ANT1', $p = 0.004$.

<https://doi.org/10.1371/journal.pntd.0009898.g005>

TRPM_{PZQ}—for simplicity referred to as AG1—was identified and validated in an orthogonal assay via single channel recording. Application of AG1 to schistosome worms *ex vivo* also caused a rapid contraction (Fig 4D). Interestingly, AG1 is not a novel chemical entity, it was previously prioritized in an earlier phenotypic screen. Mansour *et al.* executed a screen of ~300,000 compounds against larval, juvenile, and adult schistosomes [26]. AG1 (LSHTM-1507) was one of seven hits prioritized from the phenotypic screening pipeline [26] all of which displayed activity against each of the three life cycle stages, a good cytotoxicity window and structural attractiveness for further derivatization [27]. A second 'hit' from the same screen (LSHTM-1945) is a closely related chemical structure, and a third compound (LSHTM-1956) was a derivative of a mammalian TRPC6 inhibitor [28]. AG1 was also identified as an anti-schistosomal compound in previous screens of the Pathogen Box executed by independent laboratories [29]. That a phenotypic screen of ~300,000 compounds [26], inherently blind to the mode of action of many of the screened ligands, should identify one (possibly more) *Sm*.TRPM_{PZQ} activators highlights an impressive convergence of phenotypic and target-based screening methods and underscores the relevance of TRPM_{PZQ} as a druggable target. These data support the execution of a larger target-based screen to identify *Sm*.TRPM_{PZQ} activators, especially given the low hit rate for agonist discovery observed from this foundational screening effort (1 from ~16,000 compounds).

Just like PZQ, AG1 was more active against adult worms than juveniles [26], and the activity reported in phenotypic assays (IC_{50} of ~1.6 μM, [26]) mirrors the activity range for *Sm*.TRPM_{PZQ} activation *in vitro* (1.3 μM, Fig 4B). However, AG1 represents a discrete chemotype from PZQ. It is a triazolopyridine derivative and a considerably more hydrophobic ligand ($M_r = 373.4$, XLogP3-AA = 5.5, TPSA = 48.6 Å²) compared with PZQ ($M_r = 312.4$, XLogP3-AA = 2.7, TPSA = 40.6 Å²). The higher hydrophobicity of AG1 may contribute to the slower kinetics of action on intact worms *ex vivo* (Fig 4D). PZQ derivatives previously shown to activate *Sm*.TRPM_{PZQ} displayed attributes tightly clustered around those of the parent ligand (average properties of agonists with $EC_{50} < 10$ μM, $M_r = 323$, average LogP = 2.3 [9]). However, the physiochemical properties of AG1 are not dissimilar from other classes of ligands that activate human TRPM8 (hTRPM8, [23]). It is therefore exciting to have discovered a novel agonist chemotype which activates *Sm*.TRPM_{PZQ} (Fig 4). Preliminary mutagenesis data with AG1 (Fig 4B), and the similar effects of ANT1 on AG1- and PZQ-evoked *Sm*.TRPM_{PZQ} activity (Fig 5C), suggest that AG1, like PZQ, functions as an orthosteric ligand occupying the transmembrane binding pocket. Further mutagenesis work will be needed to expand these observations and resolve the relative binding poises of the two drugs. This comparison may hold significance as binding site mutants that impair PZQ binding may not necessarily impair the interaction of AG1, or other channel activators. This is known for hTRPM8 ligands [9]—for example, the conservative replacement hTRPM8[R842K] inhibits PZQ activation of hTRPM8 but has no effect on activation by cooling agent WS-12. Similarly, hTRPM8 [H845W] abolishes responses to icilin but not PZQ [9]. This could prove an important observation in the context of engaging TRPM_{PZQ} channels refractory to PZQ, for example in *Fasciola* species [9].

The screen also identified a larger number of potential *Sm*.TRPM_{PZQ} blockers (32 from 16,000 compounds), which require further investigation to define their mode of action. For

example, do these ligands act as pore blockers or as binding site antagonists? The utility of *Sm*.TRPM_{PZQ} blockers (as opposed to *Sm*.TRPM_{PZQ} activators) as anthelmintics is unproven, however their study and optimization has merit in providing selective tools for understanding worm physiology and the role of *Sm*.TRPM_{PZQ} *in vivo*. Here, we validated the blocking activity of a single of these candidates (ANT1), which antagonized PZQ action in the Ca²⁺ reporter (Fig 4F), electrophysiological (Fig 5C and 5D) and a worm contraction assay (Fig 4G). ANT1, like PZQ, contains a piperazin-1-yl methanone substructure. This structural resemblance, and the dissimilar action of ANT1 and La³⁺ on PZQ-evoked responses (Fig 5C and 5D), suggests ANT1 also acts as an orthosteric ligand.

In conclusion, this work has optimized methods for executing a highly miniaturized, large scale small molecule screen against a parasitic flatworm ion channel targeted by PZQ. Discovery of new chemotypes using these methods will help decipher features of *Sm*.TRPM_{PZQ} ligands critical for anthelmintic efficacy, and provide a workflow for screening campaigns at other parasitic flatworm ion channels.

Materials and methods

Ethics statement

All animal experiments followed ethical regulations approved by the MCW IACUC committee (AUA00006079/6476).

Reagents

Cell culture reagents were from Invitrogen. Lipofectamine 2000 was from ThermoFisher. Libraries were sourced as follows: LOPAC₁₂₈₀ (Sigma), the Pathogen Box (Medicines for Malaria), Scripps Drug Discovery Library (Scripps Institute). FLIPR Calcium 5 assay kits were from Molecular Devices. Additional supply of AG1 (3-(3,4-Dimethoxyphenyl)-6-(3-propan-2-ylphenyl)-[1,2,4]triazolo[4,3-a]pyridine; PubChem CID:122196572, C₂₃H₂₃N₃O₂) was sourced from Evotec and ANT1 (1-(9H-fluoren-9-yl)-4-(5-methyl-3-phenyl-1,2-oxazole-4-carbonyl)piperazine; PubChem CID:2813918, C₂₈H₂₅N₃O₂) was sourced from Maybridge. All other routinely used chemical reagents were purchased from Sigma.

HTS screening workflow

HEK cells were transfected with cDNA (400µg/ml DNA) encoding *Sm*.TRPM_{PZQ} using a Maxcyte STX electroporation system and incubated overnight at 37°C. This system is uniquely capable of large scale transfections providing one batch of cells ready for large scale HTS [30]. Briefly, the HEK cells were resuspended at 10⁸/ml in Maxcyte electroporation buffer. Plasmid DNA was added to the cells in buffer to achieve a concentration of 400 µg/ml from a stock of 5mg/ml (in TE buffer). This mixture was loaded into the appropriate cassette, inserted into the machine, and cells electroporated. Cells were then frozen to provide a single supply of transfected cells for all subsequent assays. On the day of the assays, cells were thawed in a 37°C waterbath, and resuspended in DMEM + 10% FBS and counted. The cells were pelleted by centrifugation at 170xg for 5 minutes. The media was aspirated, and the remaining pellet was resuspended in 1x HBSS with 20 mM HEPES and 1% DMSO to achieve 1.33x10⁶ cells/ml. This cell suspension was then dispensed at 3 µl/well to the 1536 well plates (Greiner Bio One part 789072) at a density of 4,000 cells/well. Measurements of fluorescence intensity (λ_{ex} = 470 nm, λ_{em} = 535 nm) were made using a FLIPR (Molecular Devices FLIPR Tetra). A read of basal fluorescence values was made (5s) prior to addition of compounds or controls (30 nl). In both 'agonist' and 'antagonist mode', the total assay volume was 6µl (1% DMSO). For the primary

screen, each compound was tested at a single concentration in triplicate, and responses compared on a per plate basis by evaluating the percentage response of each compound versus the 'high control' (response to EC₁₀₀ PZQ (10 μM) for the agonist screen, DMSO for the antagonist screen)) corrected for 'low control' (response to DMSO for the agonist screen, response to EC₈₀ PZQ (500 nM) in the presence of DMSO or compounds (nominally 5 μM) for the antagonist screen). Ligand performance was categorized using an algorithm based on the activity of the entire dataset to define a 'hit-cutoff' parameter for both agonist-mode and antagonist-mode screening. Any compound with greater percent activation than this cutoff was assigned as 'active' prior to titration and counter-screening. Titration assays were executed using the same reagents, protocols and detection systems, done as 10-point concentration-response curves, performed in triplicate. Counter-screening was performed using untransfected HEK293 cells for comparison with results testing the same compounds effect on cells expressing *Sm*.TRPM_{PZQ}, with ATP used as the positive control. For each compound, activity was plotted against compound concentration and data were fitted with a sigmoidal function. In order to be considered a hit at this stage a compound must achieve a EC₅₀ < 5 μM for agonists and IC₅₀ < 5 μM for antagonists. All compounds selected for titration were subjected to LC-MS analysis to confirm mass and sample purity. ChemAxon (<https://www.chemaxon.com>) academic licensing was provided for the use of Instant JChem (ver. 15.10.12.0) to perform compound mining of the libraries utilized in this effort.

Schistosome mobility assays

Adult schistosomes were harvested from the mesenteric vasculature of female Swiss Webster mice previously infected (~49 days earlier) with *S. mansoni* cercariae (NMRI strain) by the Schistosomiasis Resource Center at the Biomedical Research Institute (BRI, Rockville, MD). Harvested schistosomes were washed in RPMI 1640 supplemented with 5% heat inactivated FBS (Gibco), HEPES (25 mM) and penicillin-streptomycin (100 units/mL). After isolation, worms were incubated overnight (37°C/5% CO₂) in vented petri dishes (100x25 mm). Movement assays were performed using male and female worms in six well dishes (~5 individual worms/3ml media per well). Video recordings of worm motility (4 frames/sec) were captured using a Zeiss Discovery v20 stereomicroscope coupled to a QiCAM 12-bit cooled color CCD camera controlled by Metamorph imaging software [31].

Electrophysiology

For electrophysiological analysis, a HEK293 cell line stably expressing *Sm*.TRPM_{PZQ} [7] was generated using the Flp-In T-REx system (K650001, ThermoFisher Scientific, Carlsbad, CA). Flp-In T-REx HEK293 cells were cultured in Dulbecco's modified Eagle's medium supplemented with 10% fetal bovine serum, penicillin (100 units/ml), streptomycin (100 μg/ml), L-glutamine (290 μg/ml), blasticidin (10 μg/ml), and hydromycin B (100 μg/ml). HEK293 cells were plated onto glass coverslips and *Sm*.TRPM_{PZQ} expression induced by addition of tetracycline (2 μg/ml) to the media 24–48 hours before recording. Prior to recording, coverslips were secured within a recording chamber of an Olympus BX51WI upright microscope. Cells were bathed in a solution containing 145 mM KCl, 10 mM HEPES, 1 mM EGTA (pH 7.2, 310–315 mOsm/kg with sucrose). The pipette solution contained 140 mM LiCl, 10 mM HEPES, 1 mM EGTA (pH 7.4, 280–285 mOsm/kg with sucrose). Patch pipettes were made of borosilicate glass (BF150-110-10, Sutter Instrument, Novato, CA) pulled on a vertical puller (Narishige, Amityville, NY, Model PC-10) with resistances 8–10 MΩ. After gigaseal formation, membrane patches were excised from cells and current recorded in voltage-clamp mode in 'inside-out' configuration using a MultiClamp 700B amplifier and Digidata 1440A digitizer (Molecular

Devices, Sunnyvale, CA). Signals were filtered with an 8-pole Bessel low pass filter at 1 kHz, and sampled at 20 kHz. Open probability (P_{open}) was assessed in single channel search mode using Clampfit 10 software. All recordings were done at room temperature. Data represent mean±standard error for ≥ 3 independent experiments.

Supporting information

S1 Table. Assay performance in titration assays. Assay performance measured across 12 plates for 368 compounds in titration assays in untransfected HEK cells (counterscreen) and HEK cells expressing *Sm*.TRPM_{PZQ}. (DOCX)

S2 Table. *Sm*.TRPM_{PZQ} agonists. Data from 3 compounds prioritized after titration assays. Compound descriptors and screening data in agonist and antagonist modes in HEK cells, and HEK cells expressing *Sm*.TRPM_{PZQ} are shown. (XLSX)

S3 Table. *Sm*.TRPM_{PZQ} antagonists. Data from 32 compounds prioritized after titration assays. Compound descriptors and screening data in agonist and antagonist modes in HEK cells, and HEK cells expressing *Sm*.TRPM_{PZQ} are shown. (XLSX)

Acknowledgments

Schistosome-infected mice were provided by the NIAID Schistosomiasis Resource Center at the Biomedical Research Institute (Rockville, MD) through NIH-NIAID Contract HHSN272201000005I for distribution via BEI Resources. We thank Medicines for Malaria Venture (MMV, Switzerland) for supply of the Pathogen Box.

Author Contributions

Conceptualization: Sang-Kyu Park, Jonathan S. Marchant.

Formal analysis: Evgeny G. Chulkov, Emery Smith, Claudia M. Rohr, Nawal A. Yahya, Sang-Kyu Park.

Funding acquisition: Louis Scampavia, Timothy P. Spicer, Jonathan S. Marchant.

Investigation: Evgeny G. Chulkov, Emery Smith, Claudia M. Rohr, Nawal A. Yahya, Sang-Kyu Park.

Project administration: Jonathan S. Marchant.

Supervision: Louis Scampavia, Timothy P. Spicer, Jonathan S. Marchant.

Validation: Evgeny G. Chulkov, Emery Smith.

Visualization: Evgeny G. Chulkov, Emery Smith, Louis Scampavia, Timothy P. Spicer, Jonathan S. Marchant.

Writing – original draft: Jonathan S. Marchant.

Writing – review & editing: Evgeny G. Chulkov, Emery Smith, Louis Scampavia, Timothy P. Spicer, Jonathan S. Marchant.

References

1. Organization WH. Ending the neglect to attain the Sustainable Development Goals—A road map for neglected tropical diseases 2021–2030. World Health Organ Monogr Ser. 2020.
2. Chai JY. Praziquantel treatment in trematode and cestode infections: an update. *Infect Chemother*. 2013; 45(1):32–43. <https://doi.org/10.3947/ic.2013.45.1.32> PMID: 24265948
3. Fukushige M, Chase-Topping M, Woolhouse MEJ, Mutapi F. Efficacy of praziquantel has been maintained over four decades (from 1977 to 2018): A systematic review and meta-analysis of factors influence its efficacy. *PLoS Negl Trop Dis*. 2021; 15(3):e0009189. <https://doi.org/10.1371/journal.pntd.0009189> PMID: 33730095
4. Spangenberg T. Alternatives to Praziquantel for the Prevention and Control of Schistosomiasis. *ACS Infect Dis*. 2020. <https://doi.org/10.1021/acsinfecdis.0c00542> PMID: 32819092
5. Cupit PM, Cunningham C. What is the mechanism of action of praziquantel and how might resistance strike? *Future medicinal chemistry*. 2015; 7(6):701–5. <https://doi.org/10.4155/fmc.15.11> PMID: 25996063
6. Chan JD, Zarowiecki M, Marchant JS. Ca²⁺ channels and praziquantel: A view from the free world. *Parasitol Int*. 2013; 62(6):619–28. <https://doi.org/10.1016/j.parint.2012.12.001> PMID: 23246536
7. Park SK, Gunaratne GS, Chulkov EG, Moehring F, McCusker P, Dosa PI, et al. The anthelmintic drug praziquantel activates a schistosome transient receptor potential channel. *J Biol Chem*. 2019; 294(49):18873–80. <https://doi.org/10.1074/jbc.AC119.011093> PMID: 31653697
8. Park SK, Marchant JS. The Journey to Discovering a Flatworm Target of Praziquantel: A Long TRP. *Trends Parasitol*. 2020; 36(2):182–94. <https://doi.org/10.1016/j.pt.2019.11.002> PMID: 31787521
9. Park S-K, Friedrich L, Yahya NA, Rohr C, Chulkov EG, Maillard D, et al. Mechanism of praziquantel action at a parasitic flatworm ion channel. *bioRxiv*. 2021. <https://doi.org/10.1101/2021.03.09.434291>
10. Inoue T, Yamashita T, Agata K. Thermosensory signaling by TRPM is processed by brain serotonergic neurons to produce planarian thermotaxis. *J Neurosci*. 2014; 34(47):15701–14. <https://doi.org/10.1523/JNEUROSCI.5379-13.2014> PMID: 25411498
11. Arenas OM, Zaharieva EE, Para A, Vasquez-Doorman C, Petersen CP, Gallio M. Activation of planarian TRPA1 by reactive oxygen species reveals a conserved mechanism for animal nociception. *Nat Neurosci*. 2017; 20(12):1686–93. <https://doi.org/10.1038/s41593-017-0005-0> PMID: 29184198
12. Verma S, Kashyap SS, Robertson AP, Martin RJ. Diethylcarbamazine activates TRP channels including TRP-2 in filaria, *Brugia malayi*. *Commun Biol*. 2020; 3(1):398. <https://doi.org/10.1038/s42003-020-01128-4> PMID: 32724078
13. Wolstenholme AJ, Williamson SM, Reaves BJ. TRP channels in parasites. *Adv Exp Med Biol*. 2011; 704:359–71. https://doi.org/10.1007/978-94-007-0265-3_20 PMID: 21290306
14. Bais S, Greenberg RM. TRP channels as potential targets for antischistosomes. *International Journal for Parasitology Drugs and Drug Resistance*. 2018; 8(3):511–7. <https://doi.org/10.1016/j.ijpddr.2018.08.003> PMID: 30224169
15. Bais S, Greenberg RM. Schistosome TRP channels: An appraisal. *International Journal for Parasitology Drugs and Drug Resistance*. 2020; 13:1–7. <https://doi.org/10.1016/j.ijpddr.2020.02.002> PMID: 32250774
16. Chan JD, Grab T, Marchant JS. Kinetic profiling an abundantly expressed planarian serotonergic GPCR identifies bromocriptine as a perdurant antagonist. *International Journal for Parasitology Drugs and Drug Resistance*. 2016; 6(3):356–63. <https://doi.org/10.1016/j.ijpddr.2016.06.002> PMID: 27397764
17. Bais S, Berry CT, Liu X, Ruthel G, Freedman BD, Greenberg RM. Atypical pharmacology of schistosome TRPA1-like ion channels. *PLoS Negl Trop Dis*. 2018; 12(5):e0006495. <https://doi.org/10.1371/journal.pntd.0006495> PMID: 29746471
18. Baillargeon P, Fernandez-Vega V, Sridharan BP, Brown S, Griffin PR, Rosen H, et al. The Scripps Molecular Screening Center and Translational Research Institute. *SLAS Discov*. 2019; 24(3):386–97. <https://doi.org/10.1177/2472555218820809> PMID: 30682260
19. Zhang JH, Chung TD, Oldenburg KR. A Simple Statistical Parameter for Use in Evaluation and Validation of High Throughput Screening Assays. *J Biomol Screen*. 1999; 4(2):67–73. <https://doi.org/10.1177/108705719900400206> PMID: 10838414
20. Otsuka Y, Airola MV, Choi YM, Coant N, Snider J, Cariello C, et al. Identification of Small-Molecule Inhibitors of Neutral Ceramidase (nCDase) via Target-Based High-Throughput Screening. *SLAS Discov*. 2021; 26(1):113–21. <https://doi.org/10.1177/2472555220945283> PMID: 32734807
21. Smith E, Janovick JA, Bannister TD, Shumate J, Ganapathy V, Scampavia L, et al. Rescue of mutant gonadotropin-releasing hormone receptor function independent of cognate receptor activity. *Scientific Reports*. 2020; 10(1):10579. <https://doi.org/10.1038/s41598-020-67473-w> PMID: 32601341

22. Diver MM, Cheng Y, Julius D. Structural insights into TRPM8 inhibition and desensitization. *Science*. 2019; 365(6460):1434–40. <https://doi.org/10.1126/science.aax6672> PMID: 31488702
23. Gonzalez-Muniz R, Bonache MA, Martin-Escura C, Gomez-Monterrey I. Recent Progress in TRPM8 Modulation: An Update. *International journal of molecular sciences*. 2019; 20(11): <https://doi.org/10.3390/ijms20112618> PMID: 31141957
24. Gunaratne GS, Yahya NA, Dosa PI, Marchant JS. Activation of host transient receptor potential (TRP) channels by praziquantel stereoisomers. *PLoS Negl Trop Dis*. 2018; 12(4):e0006420. <https://doi.org/10.1371/journal.pntd.0006420> PMID: 29668703
25. Babes RM, Selescu T, Domocos D, Babes A. The anthelmintic drug praziquantel is a selective agonist of the sensory transient receptor potential melastatin type 8 channel. *Toxicol Appl Pharmacol*. 2017; 336:55–65. <https://doi.org/10.1016/j.taap.2017.10.012> PMID: 29054683
26. Mansour NR, Paveley R, Gardner JM, Bell AS, Parkinson T, Bickle Q. High Throughput Screening Identifies Novel Lead Compounds with Activity against Larval, Juvenile and Adult *Schistosoma mansoni*. *PLoS Negl Trop Dis*. 2016; 10(4):e0004659. <https://doi.org/10.1371/journal.pntd.0004659> PMID: 27128493
27. Gardner JMF, Mansour NR, Bell AS, Helmbly H, Bickle Q. The discovery of a novel series of compounds with single-dose efficacy against juvenile and adult *Schistosoma* species. *PLoS Negl Trop Dis*. 2021; 15(7):e0009490. <https://doi.org/10.1371/journal.pntd.0009490> PMID: 34280206
28. <https://pubchem.ncbi.nlm.nih.gov/bioassay/2553>
29. Maccesi M, Aguiar PHN, Pasche V, Padilla M, Suzuki BM, Montefusco S, et al. Multi-center screening of the Pathogen Box collection for schistosomiasis drug discovery. *Parasites & vectors*. 2019; 12(1):493. <https://doi.org/10.1186/s13071-019-3747-6> PMID: 31640761
30. Smith E, Davis-Gardner ME, Garcia-Ordóñez RD, Nguyen TT, Hull M, Chen E, et al. High-Throughput Screening for Drugs That Inhibit Papain-Like Protease in SARS-CoV-2. *SLAS Discov*. 2020; 25(10):1152–61. <https://doi.org/10.1177/2472555220963667> PMID: 33043784
31. Chan JD, McCorvy JD, Acharya S, Johns ME, Day TA, Roth BL, et al. A Miniaturized Screen of a *Schistosoma mansoni* Serotonergic G Protein-Coupled Receptor Identifies Novel Classes of Parasite-Selective Inhibitors. *PLoS Pathog*. 2016; 12(5):e1005651. <https://doi.org/10.1371/journal.ppat.1005651> PMID: 27187180